On Low-Pass Phase Noise Mitigation in OFDM System for mmWave Communications

Xiaoming Chen[1(✉)], Wei Fan[2], and Anxue Zhang[1]

[1] School of Electronic and Information Engineering, Xi'an Jiaotong University, Xi'an, China
{xiaoming.chen,anxuezhang}@mail.xjtu.edu.cn
[2] Department of Electronic Systems, Aalborg University, Aalborg, Denmark
wfa@es.aau.dk

Abstract. A phase noise (PN) mitigation scheme was proposed for orthogonal frequency division multiplexing (OFDM) in a previous work. The proposed scheme does not require detailed knowledge of PN statistics and can effectively compensate the PN with sufficient number of unknowns. In this paper, we analyze the performance of PN estimation/mitigation using the proposed scheme. It is shown that increasing the number of unknowns reduces the modeling error, yet increases the additive noise. Hence, increasing the number of unknowns increases the computational complexity and can even degrade the estimation performance. It is also shown that the PN spectral shape of the phase-locked-loop (PLL) based oscillator also affects the PN mitigation and that a larger PN may not necessarily degrade the performance of the OFDM system with PN mitigation. Simulations with realistic millimeter-wave (mmWave) PN and channel models are conducted to verify these findings.

Keywords: Phase noise mitigation · mmWave communications
OFDM systems

1 Introduction

The orthogonal frequency division multiplexing (OFDM) technique [1] (that has been adopted in many modern communication systems) is recently chosen to be the main waveform for 5G communications below 40 GHz and is currently considered as a strong waveform candidate for 5G communications above 40 GHz, according to the 3GPP 5G standardization [2]. In this work, we focus on OFDM systems at millimeter-wave (mmWave) frequencies [3–5].

Like other multicarrier waveforms, the OFDM system is sensitive to oscillator phase noises (PNs). PN impairments on OFDM systems have been studied intensively in the literature, e.g., [6–17]. A PN suppression scheme was proposed in [7]. The scheme suppresses the PN effect via the minimum mean square error

B. Li et al. (Eds.): ChinaCom 2017, LNICST 237, pp. 271–280, 2018.
https://doi.org/10.1007/978-3-319-78139-6_28

(MMSE) equalization with prior knowledge of additive white Gaussian noise (AWGN) and PN statistics. The authors in [8] proposed an intercarrier interference (ICI) self-cancellation scheme by modulating one symbol to two adjacent subcarriers with opposite weights. This scheme can effectively cancel the PN effect at the cost of reducing the OFDM spectral efficiency by half. An ICI correction algorithm (by estimating discrete spectral components of the PN) was proposed in [9]. The algorithm was further developed in [10] by linear interpolating between adjacent OFDM symbols, resulting in enhanced system performance at the cost of increased complexity and one extra OFDM symbol delay. Both ICI correction algorithms require iteratively processing. A non-iterative PN mitigation method (based on maximum likelihood estimation) was proposed in [11]. The method was improved by exploiting the spectral geometry of the PN [12]. Another non-iterative PN mitigation scheme with lower complexity was proposed in [13]. Joint compensation of PN and IQ imbalance was tacked in [14]. Joint estimation of PN and carrier frequency offset (CFO) was studied in [14,15]. Joint mitigation of PN, CFO, and sampling frequency offset (SFO) was investigated in [17].

The PN mitigation scheme proposed in [17] does not require detailed knowledge of PN statistics. It estimates the PN (within each OFDM symbol) at certain time or spectral anchors (unknowns), and approximate the PN by linear interpolation between time anchors or discrete Fourier transform of spectral anchors. Nevertheless, a thorough performance analysis of the scheme is missing. Therefore, in this work, we analyze the performance of the scheme. It is shown that increasing the number of anchors reduces the modeling error, yet increases the additive noise in PN estimation.

The Wiener PN of a free-running oscillator is the most popular PN model in the literature [6,7,9–17], whereas the PN of a phase-locked-loop (PLL) based oscillator (referred to as PLL PN hereafter) is used in [9] as well. The spectrum of Wiener PN has a constant decay of 20 dB/decade, whereas spectrums of PLL PNs can have different shapes, depending on the levels of different noise sources (cf. Sect. 2). Another contribution of this work is that we show that the PN's spectral shape also affects the performance of the PN mitigation scheme and that, by having suitable subcarrier spacing and anchor number, a larger PN may even result in better performance with the PN mitigation scheme (provided that most of its energy is concentrated at low offset frequencies).

Notations: Throughout this paper, *, ^{T}, ^{H}, and † denote complex conjugate, transpose, Hermitian, and Moore-Penrose pseudoinverse, respectively. Lower case bold letter ($\mathbf{x}$) and upper case bold letter ($\mathbf{X}$) represent column vector and matrix, respectively. $\mathbf{I}$ is the identity matrix. $\|\mathbf{x}\|$ is the Euclidean norm of $\mathbf{x}$. diag($\mathbf{x}$) denotes a diagonal matrix whose diagonal elements are given by $\mathbf{x}$.

2 System Model

In order to focus on PN impairments, we assume perfect time-synchronization and quasi-static multipath channel (with a channel length of L). The PN impaired signal at the receiver at the nth time sample can be expressed as

$$y(n) = \exp\left(j\phi(n)\right) \sum_{l=0}^{L-1} h_l x(n-l) + w(n) \tag{1}$$

where x represents the transmitted OFDM signal including cyclic prefix (CP), h_l ($l = 0, \cdots, L-1$) is the lth tap of the channel impulse response (CIR), w denotes the AWGN, and ϕ denotes the PN.

The Wiener PN is the most popular PN model in the literature [6,7,9–17]. It is given as

$$\phi(n+1) = \phi(n) + \eta(n) \tag{2}$$

where η is a zero-mean Gaussian random variable with variance of $4\pi f_{3\text{dB}}/f_\text{s}$ with f_s denoting the sampling frequency and $f_{3\text{dB}}$ representing the 3-dB bandwidth of the PN. As can be seen, the Wiener PN can be characterized by a single parameter, i.e., its 3-dB bandwidth $f_{3\text{dB}} = \pi\varsigma f_\text{s}^2$, where ς is a parameter that reflects the quality of the oscillator [18]. Nevertheless, the value of $f_{3\text{dB}}$ (instead of ς) is usually given in the literature.

Due to its simplicity, the Wiener PN model (2) is widely used in the literature. However, PLL-based oscillators are ubiquitously used in practical mmWave transceivers. As a result, we resort to the PLL PN in this paper.

The PLL PN consists of three main noise sources, i.e., noises from the reference oscillator θ_ref, the phase-frequency detector and the loop filter θ_LP, and the voltage controlled oscillator (VCO) θ_VCO, as shown in Fig. 1. The Laplace transform of the PN of the PLL-based oscillator is given as [19]

$$\theta_\text{out}(s) = \frac{N_\text{D} K_\text{VCO} Z(s) \left[K_\text{D}\theta_\text{ref}(s) + \theta_\text{LP}(s)\right] + sN_\text{D}\theta_\text{VCO}(s)}{sN_\text{D} + K_\text{D} K_\text{VCO} Z(s)} \tag{3}$$

where K_D denotes the gain of the phase-frequency detector, K_VCO represents the sensitivity of the VCO, $Z(s)$ represents the loop filter, and $1/N_\text{D}$ is the frequency divider. The detailed modeling parameters are listed in Table 4-2 of [19].

As can be seen from (3), θ_ref and θ_LP dominate at low (offset) frequencies, and θ_VCO dominates at high frequencies. By adjusting their levels, different spectral shapes of PN can be obtained. Figure 2 shows power spectral densities (PSDs) of

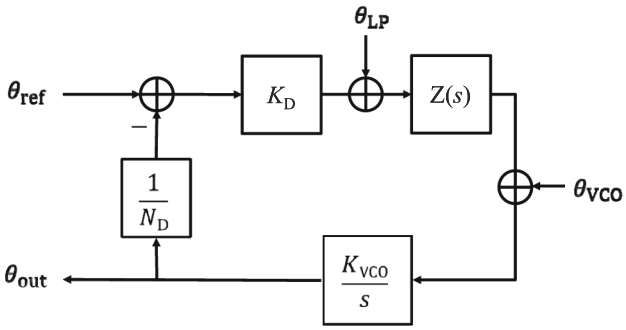

Fig. 1. Phase noise model of PLL-based oscillator.

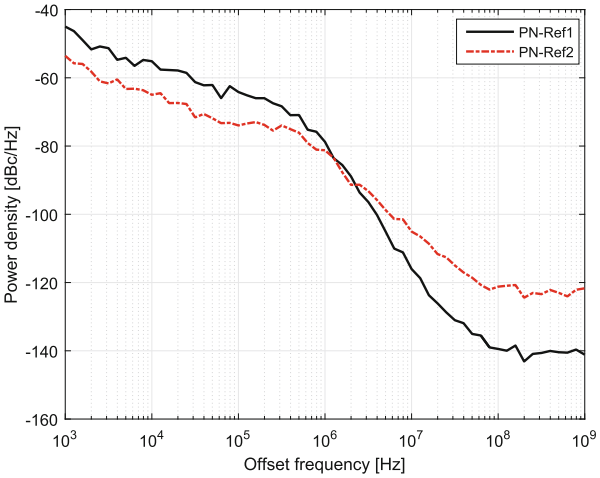

Fig. 2. PSDs of two PLL PNs. (Color figure online)

two PLL PNs at 82 GHz. The red curve (PN-Ref2) is obtained by choosing the high PN mode (see Table 4-2 of [19]). The black curve (PN-Ref1) is obtained by increasing the power of θ_{LP} by 10 dB and reducing the power of θ_{VCO} by 18 dB. The two PLL PNs are used to show the spectral shape effect on PN mitigation in Sect. 5.

3 PN Mitigation Scheme

Let $\mathbf{y} = [y(0)\ y(1)\ \cdots\ y(N-1)]^T$ be the received time-domain OFDM symbol (after CP removal), where N is the number of subcarriers. The PN is mitigated by $\mathbf{\Phi y}$, where

$$\mathbf{\Phi} = \mathrm{diag}\left\{\left[\exp\left(-j\hat{\phi}\,(0)\right)\ \cdots\ \exp\left(-j\hat{\phi}\,(N-1)\right)\right]^T\right\} \tag{4}$$

with $\hat{\phi}$ denoting the estimate of ϕ. Hence the task of PN mitigation is essentially PN estimation.

Let $\mathbf{H}_{\mathrm{p}}$ be an $N_{\mathrm{p}} \times N_{\mathrm{p}}$ diagonal matrix consisting of the channel transfer functions (CTFs) at the N_{p} pilot subcarriers ($N_{\mathrm{p}} \leq N$), $\mathbf{s}_{\mathrm{p}}$ be a vector consisting of the N_{p} subcarriers, $\mathbf{D}$ be an $N_{\mathrm{p}} \times N$ submatrix of the $N \times N$ discrete Fourier transform (DFT) matrix $\mathbf{F}$ (whose elements are given by $\exp(-j2\pi nk/N)/\sqrt{N}$, $(k,\ n = 0, \cdots, N-1)$ corresponding to the N_{p} pilot subcarriers, and $\tilde{\mathbf{w}}$ be an $N \times 1$ vector consisting of the time-domain AWGNs. Left multiplying (1) by $\mathbf{D\Phi}$, one obtains

$$\mathbf{D\Phi y} = \mathbf{H}_{\mathrm{p}}\mathbf{s}_{\mathrm{p}} + \mathbf{D\Phi}\tilde{\mathbf{w}}. \tag{5}$$

Let $\mathbf{Y} = \text{diag}(\mathbf{y})$ and $\mathbf{T}$ be an $N \times q$ transformation matrix, such that $\mathbf{\Phi} \approx \text{diag}(\mathbf{T}\boldsymbol{\alpha})$, where $\boldsymbol{\alpha}$ consists of q unknowns or anchors ($q \leq N_\text{p}$), and is given as

$$\boldsymbol{\alpha} = (\mathbf{DYT})^\dagger \mathbf{H}_\text{p}\mathbf{s}_\text{p} + (\mathbf{DYT})^\dagger \tilde{\mathbf{w}}. \tag{6}$$

The first term in the right hand side (RHS) of (6) is the least-square (LS) estimator of $\boldsymbol{\alpha}$ [15], whereas the second term in the RHS of (6) is additive noise.

The physical meaning of $\boldsymbol{\alpha}$ depends on the type of the transformation matrix. If $\mathbf{T}$ is a linear interpolation matrix [16], the elements in $\boldsymbol{\alpha}$ are estimates of the inverse carrier PN $\exp(-j\phi)$ at the q anchors (time samples). These anchors are usually evenly distributed in the time-domain OFDM symbol.

Since the PN spectrum is concentrated at low frequencies [9], $\mathbf{T}$ can be a $N \times q$ submatrix of $\mathbf{F}$, corresponding to the q lowest spectral components. In this case, the elements in $\boldsymbol{\alpha}$ are the spectral components of $\exp(-j\phi)$.

The computational complexity of the PN mitigation scheme mainly depends on the pseudoinverse of an $N_\text{p} \times q$ matrix in (6), whose complexity increases linearly with N_p, yet cubically with q [20]. In the next section, we analyze the performance of the PN mitigation/estimation with respect to (w.r.t.) q.

4 Performance Analysis

For the convenience of analysis, we study the performance of the PN mitigation/estimation in the preamble (where $N_\text{p} = N$). (As shown in Sect. 5, the findings hold for the payload as well.)

The LS estimator of the PN, i.e., the first term in the RHS of (6), contains modeling error $\mathbf{\Phi} - \text{diag}(\mathbf{T}\boldsymbol{\alpha})$. Assuming perfect estimation of $\boldsymbol{\alpha}$ (by setting the second term in the RHS of (6), i.e., the additive noise, to zero), it is self-evident that the modeling error reduces to zero as q increases to N.

Now we examine the effect of the additive noise in (6) w.r.t. q. Let $\breve{\mathbf{w}} = \mathbf{F}\mathbf{\Phi}\tilde{\mathbf{w}}$. Since $\mathbf{F}\mathbf{\Phi}$ is unitary matrix, $\breve{\mathbf{w}}$ and $\tilde{\mathbf{w}}$ have the same statistics. Thus, the additive noise in (6) can be equivalently written as

$$\mathbf{z} = (\mathbf{FYT})^\dagger \breve{\mathbf{w}} = (\mathbf{T})^\dagger (\mathbf{Y})^{-1} (\mathbf{F})^H \tilde{\mathbf{w}}. \tag{7}$$

For simplicity, we assume that $\mathbf{T}$ is the DFT transformation matrix. The power of the additive noise is given as

$$\begin{aligned} \text{E}\left[\mathbf{z}^H\mathbf{z}\right] &= \sigma_w^2 \text{E}\left\{\text{Tr}\left[(\mathbf{T})^\dagger (\mathbf{Y})^{-1}\left((\mathbf{Y})^{-1}\right)^*\left((\mathbf{T})^\dagger\right)^H\right]\right\} \\ &= \sigma_w^2 \text{E}\left\{\text{Tr}\left[\left(\mathbf{T}\mathbf{T}^H\right)^\dagger (\mathbf{Y})^{-1}\left((\mathbf{Y})^{-1}\right)^*\right]\right\} \\ &= \sigma_w^2 \frac{q}{N} \text{E}\left\{\text{Tr}\left[(\mathbf{Y})^{-1}\left((\mathbf{Y})^{-1}\right)^*\right]\right\}. \end{aligned} \tag{8}$$

Using Jensen's inequality, it is easy to show that (8) is lower bounded by $\frac{q}{N}\frac{\sigma_w^2}{\sigma_h^2\sigma_s^2+\sigma_w^2} = \frac{q}{N}\frac{1}{\gamma_0+1}$, where σ_h^2, σ_s^2, and σ_w^2 are the variances of the CIR, subcarrier symbol, and AWGN, respectively, and $\gamma_0 = \sigma_h^2\sigma_s^2/\sigma_w^2$ is the signal-to-noise-ratio (SNR). As can be seen from (8) that increasing q will increase the power

of the additive noise in (6) for fixed N and SNR. This is because that there are more anchors to estimate as q increases. All in all, for PN estimation, increasing q reduces the modeling error, yet increases the additive noises.

The PN mitigation scheme (cf. Sect. 3) is in essence a low-pass filter, which removes the PN at low (offset) frequencies. This is obvious when the DFT transformation is used, which only estimate (and remove) the q lowest spectral components. The impulse response of the linear interpolation is a triangular function, which is a convolution of two identical rectangular functions. Hence, the frequency response of the linear interpolation is the multiplication of two identical Sinc function, implying that it is also a low-pass filter. The cutoff frequency (f_{cut}) of the PN mitigation scheme approximately equals the inverse of the temporal spacing of the anchors, T/q, where T denotes the OFDM symbol duration. Thus, f_{cut} is approximately given as

$$f_{\text{cut}} \approx q/T = q f_{\text{sub}} \tag{9}$$

where f_{sub} denotes subcarrier spacing. Therefore, it is the spectral power above f_{cut} that dominates the residual PN after PN mitigation.

5 Simulations

In this section, we verify the findings of the previous section by simulations.

Figure 3 shows an example of the PN and its estimates using the PN estimation scheme with linear interpolation and DFT transformation, respectively, for an OFDM system (in an ideal channel) with $N = 512$, $N_{\text{p}} = 32$, $q = 7$, and sampling frequency of $f_{\text{s}} = 250\,\text{MHz}$. The PLL PN, PN-Ref2 (cf. Fig. 2), is used.

In order to demonstrate the effect q on PN estimation, we calculating the average MSE of the estimated PNs over 500 symbols. Figure 4 shows the MSE performance of the PN estimation as a function of q. Figure 4a corresponds to the preamble case, while Fig. 4b corresponds to the payload case with $N_{\text{p}} = 32$ scattered pilots. As can be seen, PN estimations with linear interpolation and DFT transformation has similar performances. It is also shown that MSE performances improve as q increases when $q < 15$, yet degrade as q increases when $q > 15$. This is because, when q is small, the modeling error dominates, however, as q becomes large, the additive noise begins to dominate, as shown in the previous section.

Now we investigate the PN's spectral shape effect on the PN mitigation. Since the PN estimations with linear interpolation and the DFT transformation have similar performance, we focus on the PN mitigation with linear interpolation hereafter.

The two PLL PNs, i.e., PN-Ref1 and PN-Ref2 (see Fig. 2), are used for simulations. The PN-Ref1 has higher spectral power at low (offset) frequencies and lower spectral power at high frequencies, as compared to the PN-Ref2. The PSD curves of the two PNs cross each other at 1–2 MHz frequencies. It can be seen from (9) that f_{cut} can be adjusted by varying the number of anchors and/or the subcarrier spacing.

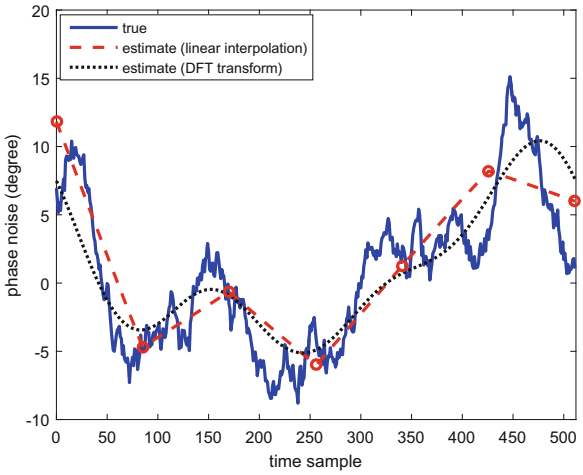

Fig. 3. Example of PN and its estimates using linear interpolation and DFT transformation within one OFDM symbol.

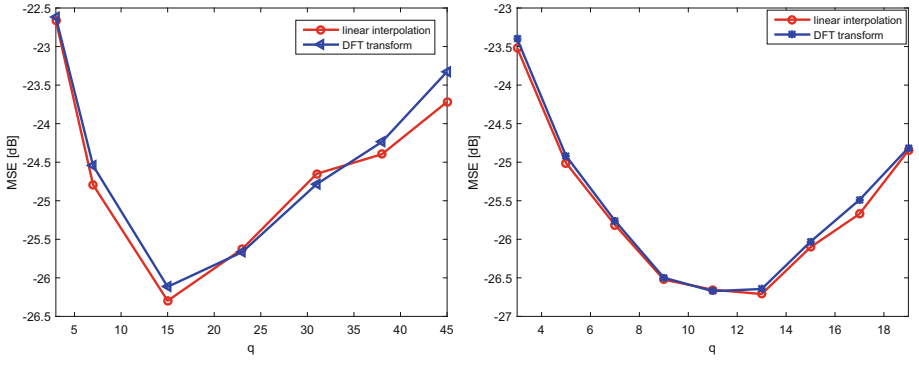

Fig. 4. MSE performances of the PN estimation using linear interpolation and DFT transformation: (a) $N_{\mathrm{p}} = N$; (b) $N_{\mathrm{p}} = 32$.

We assume an OFDM system with $N = 512$ and $N_{\mathrm{p}} = 32$. The QuaDRiGa channel model [21] (a geometry-based stochastic channel model) is used for emulating the mmWave channel at 82 GHz. In order to see the spectral shape effects of the two PNs, we conduct two sets of simulations. One with $q = 3$ and $f_{\mathrm{sub}} = 240$ kHz, so that $f_{\mathrm{cut}} = 0.72$ MHz is smaller than the crossing frequency of the two PNs. The other with $q = 7$ and $f_{\mathrm{sub}} = 480$ kHz, so that $f_{\mathrm{cut}} = 3.36$ MHz is larger than the crossing frequency of the two PNs.

Figure 5 shows the bit-error-rate (BER) performance of the OFDM system with 16-QAM, $q = 3$, and $f_{\mathrm{sub}} = 240$ kHz. As a reference, the BER performance with common phase error (CPE) correction [7] is also presented as a reference.

Figure 5a corresponds to PN-Ref1, whereas Fig. 5b corresponds to the PN-Ref2. As can be seen by comparing the BERs without PN correction, PN-Ref1 degrades the OFDM system (without PN mitigation) more than PN-Ref2 does. This is because its energy (over the whole frequency) is larger than that of PN-Ref2. Since $f_{\text{cut}} = 0.72\,\text{MHz}$ is smaller than the crossing frequency of the two PNs (i.e., PN-Ref1 has more residual energy than PN-Ref2 does after the PN mitigation), the PN-Ref1 degrades the OFDM system (with PN mitigation) more severely than PN-Ref2 does.

Figure 6 shows the BER performance of the OFDM system with 64-QAM, $q = 7$, and $f_{\text{sub}} = 480$ kHz. Figure 6a corresponds to PN-Ref1, whereas Fig. 6b

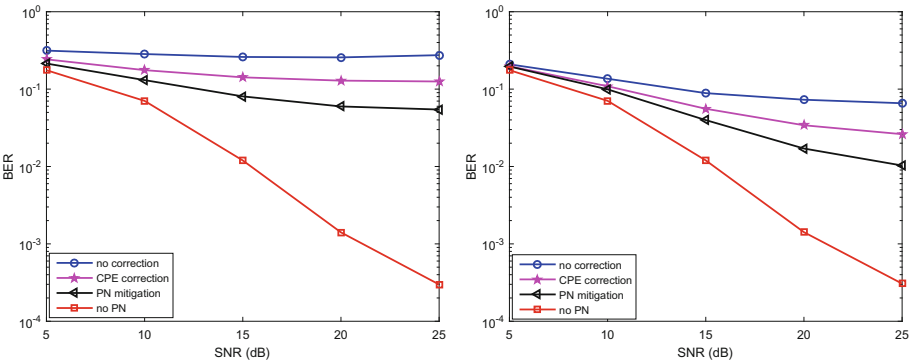

Fig. 5. BER performances of OFDM system (with 16-QAM, $f_{\text{sub}} = 240$ kHz, $q = 3$) without PN correction, with CPE correction, with PN mitigations, and without PN in mmWave multipath fading channel: (a) PN-Ref1; (b) PN-Ref2.

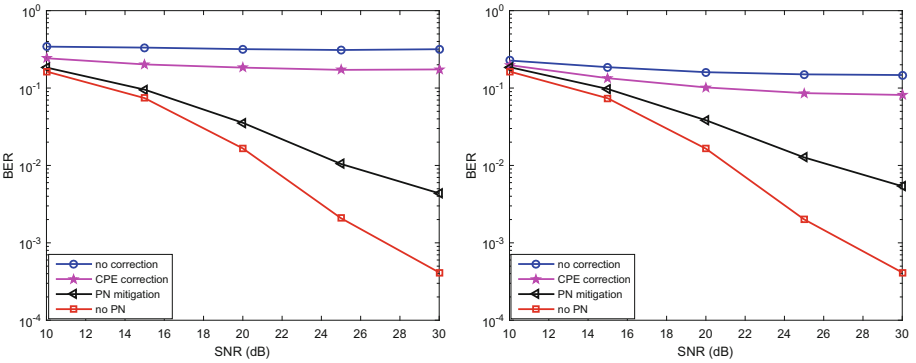

Fig. 6. BER performances of OFDM system (with 64-QAM, $f_{\text{sub}} = 480$ kHz, $q = 7$) without PN correction, with CPE correction, with PN mitigations, and without PN in mmWave multipath fading channel: (a) PN-Ref1; (b) PN-Ref2.

corresponds to PN-Ref2. As can be seen even though PN-Ref1 has larger energy than PN-Ref2, with the phase noise mitigation, the BER performance of the OFDM system in the presence of PN-Ref1 is (slightly) better than that in the presence of PN-Ref2. This is because $f_{\text{cut}} = 3.36\,\text{MHz}$ is larger than the crossing frequency of the two phase noises, and, after removing the phase noise below f_{cut} (using the phase noise mitigation), the residual PN-Ref1 is smaller than that of PN-Ref2. Comparing Figs. 5 and 6, it is safe to conclude that the spectral shape of the phase noise also affects the performance of phase noise mitigation. A larger phase noise may not necessarily degrade the performance of the OFDM system (with PN mitigation) more than a smaller PN does. It depends on the spectral shape and the cutoff frequency of the phase noise mitigation scheme.

6 Conclusion

In this paper, we studied the performance of a PN mitigation scheme for mmWave OFDM systems with realistic PN and channel models. It was shown that increasing the number of anchors reduces the modeling error, yet increases the additive noise, and therefore, may not necessarily improve the performance of PN estimation. It was also shown that the spectral shape of the PN also affects the PN mitigation, and that it is the PN's power above the cutoff frequency of the PN mitigation scheme that dominates the residual PN impairment.

References

1. Bingham, J.A.C.: Multicarrier modulation for data transmission, an idea whose time has come. IEEE Comm. Mag. **28**, 5–14 (1990)
2. 3GPP. http://www.3gpp.org/
3. Fan, W., Carton, I., Nielsen, J.Ø., Olesen, K., Pedersen, G.F.: Measured wideband characteristics of indoor channels at centimetric and millimetric bands. EURASIP J. Wirel. Commun. Netw. **2016**, 58 (2016)
4. Guan, K., Li, G., Kuerner, T., Molisch, A.F., Peng, B., He, R., Hui, B., Kim, J.H., Zhong, Z.: On millimeter wave and THz mobile radio channel for smart rail mobility. IEEE Trans. Veh. Technol. **66**, 5658–5674 (2017)
5. Ai, B., Guan, K., He, R., Li, J., Li, G., He, D., Zhong, Z.: On indoor millimeter wave massive MIMO channels: measurement and simulation. IEEE J. Sel. Areas Commun. **35**, 1678–1690 (2017)
6. Armada, A.G.: Understanding the effects of phase noise in orthogonal frequency division multiplexing (OFDM). IEEE Trans. Broadcast. **47**, 153–159 (2001)
7. Wu, S., Bar-Ness, Y.: OFDM system in the presence of phase noise: consequences and solutions. IEEE Trans. Commun. **52**, 1988–1996 (2004)
8. Zhang, J., Rohling, H., Zhang, P.: Analysis of ICI cancellation scheme in OFDM systems with phase noise. IEEE Trans. Broadcast. **50**, 97–106 (2004)
9. Petrovic, D., Rave, W., Fettweis, G.: Effects of phase noise on OFDM systems with and without PLL: characterization and compensation. IEEE Trans. Commun. **55**, 1607–1616 (2007)

10. Tchamov, N.N., Rinne, J., Hazmi, A., Valkama, M., Syrjala, V., Renfors, M.: Enchanced algorithm for digital mitigation of ICI due to phase noise in OFDM receivers. IEEE Wirel. Commun. Lett. **2**, 6–9 (2013)
11. Rabiei, P., Namgoong, W., Al-Dhahir, N.: A non-iterative technique for phase noise ICI mitigation in packet-based OFDM systems. IEEE Trans. Sig. Process. **58**, 5945–5950 (2010)
12. Mathecken, P., Riihonen, T., Werner, S., Wichman, R.: Phase noise estimation in OFDM: utilizing its associated spectral geometry. IEEE Trans. Sig. Process. **64**, 1999–2012 (2016)
13. Chen, X.: OFDM based multi-node transmission in the presence of phase noises for small cell backhaul. IEEE Commun. Lett. **21**, 1207–1210 (2017)
14. Zou, Q., Tarighat, A., Sayed, A.H.: Joint compensation of IQ imbalance and phase noies in OFDM wireless systems. IEEE Trans. Commun. **57**, 404–414 (2009)
15. Lin, D.D., Pacheco, R., Lim, T.J., Hatzinakos, D.: Joint estimation of channel response, frequency offset, phase noise in OFDM. IEEE Trans. Sig. Process. **54**, 3542–3554 (2006)
16. Salim, O.H., Nasir, A.A., Mehrpouyan, H., Xiang, W., Durrani, S., Kennedy, R.A.: Channel, phase noise, and frequency offset in OFDM systems: joint estimation, data detection, and hybrid cramer-rao lower bound. IEEE Trans. Commun. **62**, 3311–3324 (2014)
17. Chen, X., Wolfgang, A.: Phase noise mitigation in OFDM-based backhaul in the presence of channel estimation and synchronization errors. In: IEEE 83rd Vehicular Technology Conference, pp. 1–5. IEEE Press, New York (2016)
18. Demir, A., Mehrotra, A., Roychowdhury, J.: Phase noise in oscillators: a unifying theory and numerical methods for characterisation. IEEE Trans. Circ. Syst. **I**(47), 655–674 (2000)
19. Zetterberg, P., Wolfgang, A., Westlund, A.: Initial multi-node and antenna transmitter and receiver architectures and schemes. mmMAGIC Deliverable D5.1 (2016)
20. Bürgisser, P., Clausen, M., Shokrollahi, A.: Algebraic Complexity Theory. Springer, Heidelberg (1997). https://doi.org/10.1007/978-3-662-03338-8
21. Jaeckel, S., Raschkowski, L., Börner, K., Thiele, L.: QuaDRiGa: a 3-D multi-cell channel model with time evolution for enabling virtual field trials. IEEE Trans. Antennas Propag. **62**, 3242–3256 (2014)